Published OnlineFirst May 12, 2015; DOI: 10.1158/2326-6066.CIR-15-0061

Research Article

Cancer Immunology Research

Interleukin-6/STAT3 Pathway Signaling Drives an Inflammatory Phenotype in Group A Ependymoma

Andrea M. Griesinger[1,2], Rebecca J. Josephson[1], Andrew M. Donson[1,2], Jean M. Mulcahy Levy[1,2], Vladimir Amani[1,2], Diane K. Birks[2,3], Lindsey M. Hoffman[4], Steffanie L. Furtek[5], Phillip Reigan[5], Michael H. Handler[2,3], Rajeev Vibhakar[1,2], and Nicholas K. Foreman[1,2,3]

Abstract

Ependymoma (EPN) in childhood is a brain tumor with substantial mortality. Inflammatory response has been identified as a molecular signature of high-risk Group A EPN. To better understand the biology of this phenotype and aid therapeutic development, transcriptomic data from Group A and B EPN patient tumor samples, and additional malignant and normal brain data, were analyzed to identify the mechanism underlying EPN Group A inflammation. Enrichment of IL6 and STAT3 pathway genes were found to distinguish Group A EPN from Group B EPN and other brain tumors, implicating an IL6 activation of STAT3 mechanism. EPN tumor cell growth was shown to be dependent on STAT3 activity, as demonstrated using shRNA knockdown and pharmacologic inhibition of STAT3 that blocked proliferation and induced apoptosis. The inflammatory factors secreted by EPN tumor cells were shown to reprogram myeloid cells, and this paracrine effect was characterized by a significant increase in pSTAT3 and IL8 secretion. Myeloid polarization was shown to be dependent on tumor secretion of IL6, and these effects could be reversed using IL6-neutralizing antibody or IL6 receptor–targeted therapeutic antibody tocilizumab. Polarized myeloid cell production of IL8 drove unpolarized myeloid cells to upregulate CD163 and to produce a number of proinflammatory cytokines. Collectively, these findings indicate that constitutive IL6/STAT3 pathway activation is important in driving tumor growth and inflammatory cross-talk with myeloid cells within the Group A EPN microenvironment. Effective design of Group A–targeted therapy for children with EPN may require reversal of this potentially immunosuppressive and protumor pathway.
Cancer Immunol Res; 3(10); 1165–74. ©2015 AACR.

Introduction

Molecular subgroups of primary ependymoma (EPN) have recently been defined, including two main EPN subgroups arising in the posterior fossa, termed Groups A and B, that confer different biologic phenotypes and clinical courses (1–3). Phenotypically, Group A tumors occur in younger children and are characterized by upregulation of a variety of pathways, including angiogenesis, mesenchymal cell differentiation, cell proliferation, and inflammatory response, that are hallmarks of aggressive tumor biology. Group A designation confers increased recurrence risk and poorer overall outcome. The difference in outcome for Group A and Group B tumors is seen at relapse where most Group B patients can be salvaged by surgery and radiation while most Group A patients will go on to subsequent relapses, which almost invariably results in death (3). Group B tumors generally occur in adolescents and young adults and overexpress genes involved in ciliogenesis, microtubule assembly, and oxidative metabolism.

A recent study by our group identified inflammatory response as the predominant ontology distinguishing Group A from Group B tumors at presentation [normalized enrichment score (NES) = 3.98; false discovery rate (FDR) q-value < 0.001; ref. 3]. Upregulation of inflammatory genes was also seen in independent Group A cohorts (1, 2). In the original study that delineated posterior fossa EPN into Groups A and B, inflammatory response genes were significantly enriched in the Heidelberg-cohort Group A tumors (NES = 1.93; FDR q = 0.016; ref. 1). A second independent study also identified inflammatory response as the second highest enriched geneset in Group A EPN (FDR q < 0.0005; ref. 2). It is widely accepted that many tumors arise from and are promoted by an inflammatory microenvironment (4, 5). This hallmark of cancer is thought to be tumorigenic in part due to suppression of host antitumor immunity. Accordingly, support for the existence of an immunosuppressive phenotype in Group A EPN was previously demonstrated by the identification of an exhausted phenotype in tumor-infiltrating T cells (3). Abrogation of

[1]Department of Pediatrics, University of Colorado Denver, Aurora, Colorado. [2]Children's Hospital Colorado, Aurora, Colorado. [3]Department of Neurosurgery, University of Colorado Denver, Aurora, Colorado. [4]Department of Cancer and Blood Diseases, Cincinnati Children's Hospital Medical Center, Cincinnati, Ohio. [5]Department of Pharmacology, University of Colorado Anschutz Medical Campus, Aurora, Colorado.

Note: Supplementary data for this article are available at Cancer Immunology Research Online (http://cancerimmunolres.aacrjournals.org/).

Corresponding Author: Andrea M. Griesinger, University of Colorado Denver at Anschutz Medical Campus, Pediatrics Department, Mail Stop 8302, 12800 E. 19th Avenue, Aurora, CO 80045. Phone: 303-724-6554; Fax: 303-724-3363; E-mail: andrea.griesinger@ucdenver.edu

doi: 10.1158/2326-6066.CIR-15-0061

Published OnlineFirst May 12, 2015; DOI: 10.1158/2326-6066.CIR-15-0061

detrimental immune phenotypes in cancer has now emerged as a novel goal for experimental therapeutic approaches (6). To identify similar clinical approaches for refractory Group A EPN, this study sought to identify the mechanism driving the inflammatory phenotype of these tumors. We show that a potential molecular mechanism underlying Group A EPN inflammatory phenotype is constitutive activation of the IL6/STAT3 pathway and cross-talk between tumor and immune cells within the tumor microenvironment (TME).

Our study is the first to identify persistent IL6/STAT3 activation as a driver of tumor growth and an associated inflammatory microenvironment in Group A EPN. Targeting the IL6/STAT3 pathway, either directly or by modifying the proinflammatory microenvironment, is a potential therapeutic approach to improve patient survival and outcomes in this deadly tumor of childhood.

Materials and Methods

Transcriptomic analysis

The primary EPN study cohort consisted of 21 primary Group A and 20 primary Group B posterior fossa EPN and 9 supratentorial EPN. A broader transcriptomic analyses utilized EPN samples obtained at relapse (8 Group A and 6 Group B) and other pediatric and adult brain tumors. This consisted of 17 atypical teratoid/rhabdoid tumors (AT/RT); 14 pediatric and 7 adult high-grade gliomas (HGG); 8 sonic hedgehog, 5 Group 3 and 7 Group 4 medulloblastomas (MED); and 15 pilocytic astrocytoma (PA). Normal brain samples ($n = 13$) were also included in this analysis, obtained from autopsy and epilepsy surgery from both infra- and supratentorial anatomic sites. All patient samples were obtained with consent (COMIRB 95-500). Tumor samples were processed identically at our institution and analyzed using the Human Genome U133plus2 Array (Affymetrix) platform as described previously (3). Microarray. CEL datafiles were background corrected and normalized using the guanine cytosine robust multi array average (gcRMA) algorithm resulting in $\log_2$ expression values (7). To reduce error associated with multiple testing, a filtered list was created containing the highest expressed probe across all samples for each gene that possessed multiple probe sets. This list was further filtered to remove probe sets that were expressed below a threshold level that denoted absence of expression in any sample. These microarray data have been deposited in the National Center for Biotechnology Information Gene Expression Omnibus (GEO) database (8) and are publicly accessible through GEO Series accession number GSE66354 (http://www.ncbi.nlm.nih.gov/geo/query/acc.cgi?acc=GSE66354). Primary EPN were assigned to consensus molecular subgroups using nonnegative matrix factorization (NMF) available through the Broad Institute Gene Pattern platform (Supplementary Fig. S1; ref. 9).

Geneset enrichment analysis (GSEA) was used to examine enrichment of genes in predefined reference sets that are based on biologic knowledge using tools available from the Broad Institute Molecular Signatures Database (MSigDB; http://www.broadinstitute.org/gsea/msigdb; ref. 10).

Tumor versus myeloid cell transcriptome analysis

To determine the distribution of transcripts of interest between tumor cells and tumor-associated myeloid cells, we performed transcriptomic analysis on populations that had been isolated from patient surgical samples by tissue disaggregation and flow cytometric sorting as described previously (3). Briefly, resected tumor was finely minced with a razor and further triturated by vigorous pipetting. A single-cell suspension was obtained by passing the sample through a 70-μm cell strainer (Becton Dickinson) of sufficiently large pore size to permit passage of all immune and tumor cells but not clumped tumor cells. Disaggregated cells were viably frozen in standard freezing media containing 10% DMSO and stored in liquid nitrogen for subsequent analysis. Isolation of tumor and myeloid subpopulations was performed by staining disaggregated samples with anti–CD45-FITC and anti–CD11b-APC antibodies (Becton Dickinson clones 2D1 and ICRF44, respectively) followed by flow sorting using a Beckman-Coulter MoFlo XDP-100. RNA was isolated from sorted cells using a microRNeasy kit (Qiagen). Extracted RNA was amplified using the Nugen WT-Ovation One-Direct System (NuGEN Technologies) that reverse transcribes RNA to cDNA, which is amplified during SPIA amplification, a linear isothermal DNA amplification process resulting in end-products of single-strand DNA. Amplified RNA was labeled (NuGEN Encore Biotin Module) and hybridized to Affymetrix Human Genome U133plus2 chips. Microarray. CEL file data were normalized as described above.

Cytokine release assay

Viably frozen disaggregated tumor samples were thawed and flow sorted to separate immune cells from tumor cells as previously described (3). Tumor cells were cultured in 1 mL optimem media supplemented with 15% FBS (O15) for 96 hours on ultra-low attachment plates. Media were harvest and immediately frozen at −80°C for later use. A high sensitivity Milliplex Map kit (Millipore) was used to measure the concentration of 13 common cytokines [GM-CSF, IFNγ, IL1β, IL2, IL4, IL5, IL6, IL7, IL8, IL10, IL12 (p70), IL13, and TNFα) as per the manufacturer's instructions. IL6 secretion in media from cell lines was also measured using Quantikine ELISA human IL6 (R&D Systems) according to the manufacturer's instructions.

Western immunoblots

Primary antibodies used were pSTAT3 (Tyr-705; cat# 9145 clone D3A7), STAT3 (cat# 9139 clone 124H6), suppressor of cytokine signaling 3 (SOCS3; cat# 2923), myeloid cell leukemia sequence 1 (BCL2-related; MCL1; cat# 5453 clone D35A5; Cell Signaling Technologies). Anti–β-actin (cat# 12262 clone 8H10D10; Cell Signaling Technologies) was used as the protein loading control. Membranes were blocked in TBS-Tween 5% milk or BSA depending on the manufacturer's recommendation. Bands were visualized with Immobilon Western Chemiluminescent HRP substrate (Millipore) on X-ray film, and densitometry measurements were performed. All experiments were performed three times, and representative blots are shown.

Cell lines

EPN cell line 811 was established from the fourth recurrence in a patient with metastatic anaplastic EPN that exhibited a Group A phenotype. This unique cell line is positive for chromosome 1q gain (1q+) as was the tumor. 1q+ is known to be a poor risk factor for EPN. This cell line was maintained under normal culture conditions in Optimem media supplemented with 15% FBS (O15; Invitrogen). Patient samples were obtained with consent (COMIRB#95-500). Glioblastoma (GBM) cell line U87, obtained

from ATCC, was cultured in MEM supplemented with 10% FBS, nonessential amino acids, sodium pyruvate, and sodium bicarbonate. Conditioned media (CM) from cell lines, as used for characterization of cytokine release and monocyte polarization, were obtained by harvesting media from a known number of cells after 24-hour incubation. Cell line authentication was performed using short tandem repeat profiling and comparison with known cell line DNA profiles.

shRNA transfection

A pLKO system (Sigma-Aldrich) was utilized for lentiviral RNAi-mediated STAT3 protein knockdown. TRC numbers for shRNAs used STAT3 TRCN0000020839, STAT3 TRCN0000020840, STAT3 TRCN0000020842 or pLKO.1 nontargeting (SHC016). Virus was removed from cells after 24-hour incubation. Validation of STAT3 knockdown was performed by Western blot analysis of cells treated identically alongside MTS, tritiated (3H)-thymidine uptake, and apoptosis assays.

MTS assay

Cells were seeded at 4,000 cells per well in 96-well plates (Corning) in antibiotic-free medium and treated with drug or lentiviral solution the next day. S3I-201 was used to inhibit STAT3 in 811. S3I-201 (Selleck Chemicals) inhibits STAT3:STAT3 complex formation and STAT3 DNA-binding and transcriptional activity and in the original paper inhibited the growth of breast cancer *in vivo* (11). Cell viability was measured using the MTS assay with CellTiter 96 AQueous One Solution Reagent (Promega) following the manufacturer's protocol 72 hours after drug treatment or 5 days after virus removal. Optical density of each well was measured with a Synergy 2 microplate reader (Biotek) at 490 nm. The proportion of cells per treatment group was normalized to control wells of DMSO control-treated cells or sh nontargeting (NT) control.

3H-thymidine uptake

Cell proliferation as determined by rate of DNA synthesis was measured by 3H-thymidine incorporation. Cells were plated in 96-well plates and treated with a dose range of S3I-201 in triplicate as described above. Twenty hours after treatment, each well was pulsed with 0.5 mCi 3H-thymidine, and the plates were incubated at 37°C for 4 hours before cell harvest. For shRNA transfections, lentivirus was added to cells as above, and 3H-thymidine was added 5 days after virus removal. Wells were washed with PBS, and 6% trichloroacetic acid was added to each well. Wells were washed with 1 mL cold 6% trichloroacetic acid after incubation for 1 hour at 4°C. The acid precipitate was dissolved overnight in 50 μL 0.5N NaOH and transferred to scintillation vials containing 3 mL of ScintiSafe-30%. Incorporated radioactivity was measured using a scintillation counter. Mitomycin C blocks proliferation and was used as a negative control for 3H-thymidine incorporation.

IncuCyte apoptosis analysis

Cells were transfected with nuclear locating signal mCherry (NLS-mCh) virus and antibiotic selected for NLS-mCh$^+$ cells. Cells were seeded at 4,000 cells per well in 96-well plates in media. Cells were cultured at 37°C and 5% CO^2 and monitored using an Incucyte Zoom (Essen BioScience). CellEvent Caspase-3/7 Green Detection Reagent (Life Technologies) was added the next day, and baseline images were taken using 10× objective. For lentiviral knockdown, caspase reagent was added following virus removal. S3I-201 was added after initial baseline images. Images were captured at 4-hour intervals from 4 separate regions per well using a 10× objective over 72 hours. Each experiment was done in triplicate, and accumulation of caspase 3/7 over time was normalized to confluence of cells.

Monocyte polarization assays

CD14$^+$ monocytes were isolated from HLA-matched donor peripheral blood by flow sorting using CD14-FITC (Becton Dickinson) and Moflo Astrios EQ flow cytometry sorter. Post-sorted cells were incubated in various conditions for 96 hours on ultra-low attachment plates (Corning). 811-conditioned media (811 CM) were collected off 90% confluent 811 cell line and immediately frozen at −80°C for later use. IL6-neutralizing antibody (R& D Systems) was used at concentration of 50 μg/mL, and tocilizumab (Genentech) was used at concentration of 1 mg/mL. Media were harvested from cells after 96 hours, and cytokine concentrations were measured by multiplex bead cytokine analysis as described above. Cells were stained with pSTAT3-PE (BD) according to the manufacturer's instructions and run on Beckman Coulter Gallios 561; analysis was done using FlowJo v10.0.7 (FlowJo).

IL8 functional assay

Media were harvested from 811-polarized monocytes (MonoCM) or nonpolarized monocytes (MonoO15) as described above. Fresh CD14$^+$ monocytes were then incubated in MonoCM or MonoO15 for 96 hours. IL8-neutralizing antibody (R&D Systems) was added to MonoCM at 5 μg/mL. Cells were collected and myeloid phenotype cell surface markers CD163, HLA-DR, and CD64 were analyzed by flow cytometry as previously described (12). Media were harvested and cytokine concentrations were measured as described above. Cytokine concentrations from primed media were subtracted to assess additional secretion.

Statistical analyses

Statistical analyses were performed using R bioinformatics, Prism (GraphPad), and Excel (Microsoft) software. For all tests, statistical significance was defined as $P < 0.05$.

Results

STAT3-upregulated genes and IL6 signaling pathway genesets are significantly enriched in Group A EPN

We used nonbiased GSEA analysis to identify transcription factor activity that might mechanistically underlie the Group A inflammatory response phenotype. Primary EPN Group A ($n = 21$) and B ($n = 20$) transcriptomic profiles were screened for enrichment of transcriptional programs using MSigDB C3 TFT (transcription factor targets) v.4 motif genesets ($n = 615$) containing genes that share a transcription factor–binding site motif defined in the TRANSFAC database (version 7.4, http://www.gene-regulation.com/). In Group A EPN, transcription factor target genes of leading cancer inflammatory mediator STAT3 (MSigDB: V$STAT3_01) were the second most enriched of 615 TFT genesets (NES = 2.07; FDR q < 0.0001; Table 1; Supplementary Fig. S2A). Specific STAT3 TFT motif–containing genes highly upregulated (fold change, FC > 10) in Group A include chemokine (C-C motif) ligand 2 (*CCL2*) and v-maf musculoaponeurotic fibrosarcoma oncogene homolog F (*MAFF*; Table 2).

Published OnlineFirst May 12, 2015; DOI: 10.1158/2326-6066.CIR-15-0061

Table 1. Enriched genesets in Group A EPN using GSEA analysis[a]

Name	NES	NOM *P*	FDR *q*	FWER *P*
MSigDB C3: motif genesets: transcription factor targets				
GGGNNTTTCC_V$NFKB_Q6_01	2.16	<0.0001	<0.0001	<0.0001
V$STAT3_01	2.06	<0.0001	<0.0001	<0.0001
V$NFKAPPAB_01	1.99	<0.0001	0.000468	0.001
TGASTMAGC_V$NFE2_01	1.96	<0.0001	0.000351	0.001
V$SRF_01	1.93	<0.0001	0.000281	0.001
V$NFKB_Q6_01	1.93	<0.0001	0.000234	0.001
V$NFKB_C	1.92	<0.0001	0.000201	0.001
V$PEA3_Q6	1.90	<0.0001	0.000176	0.001
V$CREL_01	1.90	<0.0001	0.000156	0.001
V$AP1_Q4	1.89	<0.0001	0.000140	0.001
Experimentally determined STAT3 geneset				
STAT3-upregulated (Yu et al., ref. 13)	2.33	<0.0001	<0.0001	<0.0001
MSigDB C2: curated genesets: BioCarta				
BIOCARTA_NKT_PATHWAY	1.97	<0.0001	0.00684	0.00400
BIOCARTA_INFLAM_PATHWAY	1.95	<0.0001	0.00342	0.00400
BIOCARTA_PML_PATHWAY	1.92	<0.0001	0.00290	0.00500
BIOCARTA_LAIR_PATHWAY	1.86	<0.0001	0.0124	0.0270
BIOCARTA_KERATINOCYTE_PATHWAY	1.83	0.00338	0.0191	0.0540
BIOCARTA_COMP_PATHWAY	1.82	<0.0001	0.0168	0.0570
BIOCARTA_IL2RB_PATHWAY	1.82	0.00166	0.0146	0.0570
BIOCARTA_CDMAC_PATHWAY	1.82	<0.0001	0.0149	0.0660
BIOCARTA_IL6_PATHWAY	1.81	<0.0001	0.0155	0.0770
BIOCARTA_NFKB_PATHWAY	1.80	0.00337	0.0158	0.0870

Abbreviations: FWER, family-wise error rate; NOM, nominal.

[a]The top 10 enriched genesets as ranked by NES are shown for transcription factor target motif and BioCarta genesets.

We further characterized the involvement of STAT3 in Group A EPN by using GSEA to measure enrichment of experimentally determined STAT3-upregulated geneset ($n = 36$), created from a review of the role of STAT3 in cancer inflammation and immunity (ref. 13; Supplementary Table S1). This geneset was enriched in Group A to a greater extent (NES = 2.33; FDR $q < 0.001$) than the STAT3 TFT geneset (Table 1; Supplementary Fig. S2B). Experimentally determined STAT3-upregulated genes in Group A (Table 2) were largely discrete from those identified as STAT3 TFTs with the exception of *CCL2* and *ICAM1*. Notable STAT3-upregulated genes (FC > 10) in Group A include chitinase 3-like 1 (*CHI3L1*, AKA *YKL-40*), *IL8*, *CCL2*, *SOCS3*, *IL6*, and prostaglandin-endoperoxide synthase 2 (*PTGS2*, AKA *COX-2*). Collectively, these data suggest activation of the STAT3 signaling pathway in Group A EPN.

It is known that IL6 drives oncogenic activation of STAT3, increasing cell proliferation, survival, and invasion while suppressing antitumor immunity (13). Persistent IL6/STAT3 pathway activation is involved in various inflammation-associated cancers, most notably colorectal (14), gastric (15), and liver (16) cancers. Given the high level of *IL6* gene expression, we hypothesized that IL6 may be driving activation of STAT3 in Group A EPN. Enrichment of MSigDB C2 BioCarta pathway v.4–curated genesets ($n = 217$; http://www.biocarta.com/genes/index.asp) was assessed using GSEA and showed that, in agreement with our hypothesis, the BioCarta IL6 pathway geneset was among the 10 highest enriched pathways in Group A (NES = 1.81; FDR q = 0.015; Tables 1 and 2; Supplementary Fig. S2C). Of note, the BioCarta cytokines and inflammatory response geneset (BIOCARTA_INFLAM_PATHWAY) was the second most enriched BioCarta pathway geneset (NES = 1.95; FDR q = 0.0034; Supplementary Fig. S2D).

A broader examination of Group A EPN–associated IL6/STAT3 pathway genes identified by GSEA gene expression was next performed in EPN from recurrences and supratentorial sites, as well as other common pediatric and adult brain tumors and normal brain. Recurrent Group A EPN showed reduced expression of *IL6*, consistent with the decreased inflammatory phenotype observed at recurrence that was previously identified (3). *IL6* expression was significantly higher in primary Group A EPN than in all other brain tumor types (Fig. 1A). *IL6* expression was higher in Group A EPN than in both adult GBM (FC = 7.0; $P = 0.039$) and MED (FC = 16.5; $P = 2.5 \times 10^{-6}$), which is notable as constitutive IL6/STAT3 activation has been identified in these tumor types (17, 18).

Similar to *IL6*, *IL8* was significantly overexpressed compared with recurrent Group A EPN (FC = 7.6, $P = 0.0016$), with all other brain tumor types (FC = 22-fold higher than all other tumor samples combined; $P = 4.3 \times 10^{-11}$), and with normal brain [(NB) FC = 104; $P = 1.4 \times 10^{-13}$; Fig. 1B]. Thus, overexpression of key inflammatory mediators *IL6* and *IL8* appears to be hallmarks of the Group A EPN transcriptome in the context of not only EPNs as a whole, but of all brain tumors. The apparent restriction of *IL6* and *IL8* gene expression to Group A EPN in this broad transcriptomic analysis provides further evidence that an IL6/STAT3 signaling pathway underlies the inflammatory signaling pathway present in Group A EPN.

Key Group A EPN IL6/STAT3 inflammation signature genes are differentially distributed between tumor and tumor-infiltrating myeloid cells

Prior studies of EPN immunobiology have identified that tumor-infiltrating immune cells can significantly contribute to the overall gene expression profiles of surgical tumor samples (19). A subset of genes associated with longer progression-free survival in EPN were found to be restricted to tumor-infiltrating myeloid cells that contribute up to 25% of the cellular content of surgical tumor specimens (12). The contribution of tumor-infiltrating myeloid cells to the inflammatory TME, through the IL6/STAT3 activation, is well established (13, 20). We, therefore, sought to determine the contribution of tumor-infiltrating

Published OnlineFirst May 12, 2015; DOI: 10.1158/2326-6066.CIR-15-0061

Table 2. Significantly upregulated genes in Group A EPN from enriched STAT3 and IL6 pathway genesets

Gene symbol	Gene title	FC	*P*	*q*
MSigDB C3: motif genesets: transcription factor targets: V$STAT3_01 genes				
CCL2	Chemokine (C-C motif) ligand 2	21.62	1.39E−08	3.67E−06
IRF1	Interferon regulatory factor 1	8.66	8.48E−08	1.11E−05
ICAM1	Intercellular adhesion molecule 1	8.32	2.11E−07	2.00E−05
MAFF	v-maf musculoaponeurotic fibrosarcoma oncogene homolog F (avian)	15.87	7.78E−07	5.19E−05
SERPING1	Serpin peptidase inhibitor, clade G (C1 inhibitor), member 1	3.11	6.45E−06	0.000264
CISH	Cytokine inducible SH2-containing protein	2.24	2.45E−05	0.000737
APBA1	Amyloid beta (A4) precursor protein-binding, family A, member 1	1.93	0.00496	0.0393
Experimentally determined STAT3-upregulated genes (Yu et al., ref. 13)				
IL8	Interleukin 8	24.13	5.22E−09	2.17E−06
CCL2	Chemokine (C-C motif) ligand 2	21.62	1.39E−08	3.67E−06
SOCS3	Suppressor of cytokine signaling 3	14.61	1.88E−08	4.35E−06
TIMP1	TIMP metallopeptidase inhibitor 1	5.49	3.65E−08	6.76E−06
ICAM1	Intercellular adhesion molecule 1	8.32	2.11E−07	2E−05
CHI3L1	Chitinase 3-like 1 (cartilage glycoprotein-39); YKL-40	40.27	2.87E−07	2.51E−05
VEGFA	Vascular endothelial growth factor A	4.71	9.77E−07	6.07E−05
PTGS2	Prostaglandin-endoperoxide synthase 2 (prostaglandin G/H synthase and cyclooxygenase); COX-2	10.57	2.82E−06	0.000142
STAT3	Signal transducer and activator of transcription 3 (acute-phase response factor)	1.63	3.72E−06	0.000176
MCL1	Myeloid cell leukemia sequence 1 (BCL2-related)	1.65	7.74E−06	0.00031
VIM	Vimentin	1.41	8.05E−06	0.000318
IL6	Interleukin 6 (interferon, beta 2)	13.41	1.02E−05	0.000381
BIRC3	Baculoviral IAP repeat-containing 3	5.94	6.29E−05	0.001533
MMP9	Matrix metallopeptidase 9 (gelatinase B, 92-kDa gelatinase, 92-kDa type IV collagenase)	7.96	6.32E−05	0.00154
JAK3	Janus kinase 3	3.56	6.54E−05	0.00157
CXCL10	Chemokine (C-X-C motif) ligand 10	7.40	0.000143	0.00281
LIF	Leukemia inhibitory factor (cholinergic differentiation factor)	3.88	0.000153	0.00298
MMP2	Matrix metallopeptidase 2 (gelatinase A, 72-kDa gelatinase, 72-kDa type IV collagenase)	2.59	0.00111	0.0134
CCL5	Chemokine (C-C motif) ligand 5	2.28	0.00405	0.0340
MYC	v-myc myelocytomatosis viral oncogene homolog (avian)	2.09	0.00414	0.0345
IL1B	Interleukin 1, beta	3.10	0.0064	0.0474
MSigDB C2: curated genesets: BioCarta: IL6_PATHWAY genes				
MAP2K1	Mitogen-activated protein kinase kinase 1	1.80	3.65E−06	0.000174
STAT3	Signal transducer and activator of transcription 3 (acute-phase response factor)	1.63	3.72E−06	0.000176
SHC1	SHC (Src homology 2 domain containing) transforming protein 1	2.51	5.35E−06	0.000226
IL6	Interleukin 6 (interferon, beta 2)	13.41	1.02E−05	0.000381
CEBPB	CCAAT/enhancer binding protein (C/EBP), beta	2.01	4.38E−05	0.00114
JAK3	Janus kinase 3	3.56	6.54E−05	0.00157
ELK1	ELK1, member of ETS oncogene family	1.42	0.000123	0.00251
SRF	Serum response factor (c-fos serum response element-binding transcription factor)	1.77	0.000234	0.00409
MAPK3	Mitogen-activated protein kinase 3	1.53	0.000782	0.0104
JUN	jun proto-oncogene	1.70	0.000952	0.0120
FOS	FBJ murine osteosarcoma viral oncogene homolog	3.99	0.00140	0.0159

myeloid cells to the Group A EPN *IL6/STAT3* gene expression signature. Surgical samples from two posterior fossa EPNs were disaggregated and flow-sorted to isolate myeloid cells ($CD45^+$, $CD11b^+$) and tumor cells ($CD45^-$). Transcriptomic analysis was performed, and the relative expression of Group A IL6/STAT3 inflammation signature genes between these TME cellular compartments was measured (Supplementary Fig. S3). Of the 34 genes identified by GSEA as enriched in the STAT3 TFT, STAT3-upregulated and IL6 pathway genesets (Table 2), *IL8*, *ICAM1*, *PTGS2*, and *IL1B* were on average more than 10-fold higher in the myeloid than in the tumor cell compartments. Conversely, *CHI3L1* gene expression was 67-fold higher in the tumor compartment. CHI3L1 has a proposed role in driving the Group A EPN–specific mesenchymal phenotype (2). Thus, tumor-infiltrating myeloid cells contribute to the IL6/STAT3 inflammatory gene expression signature in the Group A EPN.

Tumor cell secretion of IL6 is associated with STAT3 phosphorylation in Group A EPN

We isolated viable tumor cells, excluding other cells in the TME, from EPN clinical samples (7 Group A; 8 Group B) by tissue disaggregation and flow sorting to remove all immune cell types as described above. Tumor cells were cultured in 1 mL serum-supplemented media (O15) for 96 hours. Multiplexed cytokine profiling revealed that IL6 was the only cytokine that was significantly higher in Group A versus Group B EPN (FC = 3.5; $P = 0.031$; Fig. 2A). Of the remaining cytokines, only IL10 was >2-fold higher in Group A than in Group B with a trend toward significance ($P = 0.12$; Supplementary Fig. S4).

Presence of significantly higher *STAT3* transcripts and STAT3-regulated transcripts is evidence of STAT3 activity; hence, we evaluated STAT3 phosphorylation as a more direct indicator of STAT3 activity in EPN patient samples. Phosphorylation of STAT3-Tyrosine 705 by upstream signaling results in dimerization and translocation to the nucleus, resulting in transcription of STAT3-target genes. The ratio of tyrosine 705-phosphorylated (pSTAT3) to total STAT3 protein, as measured by Western blot analysis, was used as a measure of STAT3 activity in patient tumor samples (12 Group A; 12 Group B; Fig. 2B shows a representative blot). Densitometric quantification of pSTAT3 and total STAT3 revealed a significantly higher ratio of phosphorylation in Group A (FC = 1.84; $P = 0.011$; Fig. 2C).

Published OnlineFirst May 12, 2015; DOI: 10.1158/2326-6066.CIR-15-0061

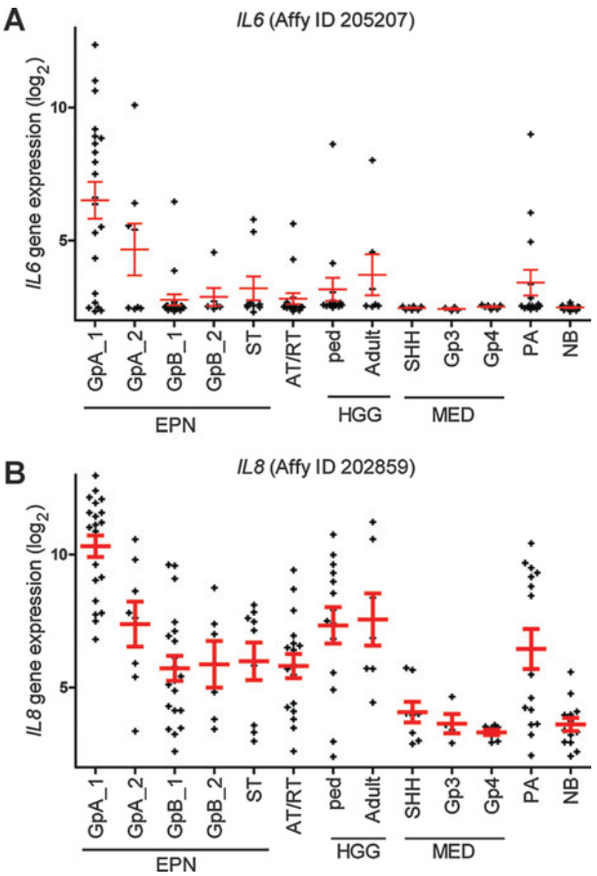

Figure 1.
Key inflammatory cytokine genes *IL6* and *IL8* are upregulated in Group A EPN versus a broad range of brain tumors and normal brain tissues. A, *IL6* and B, *IL8* in Group A EPN compared with recurrent EPN specimens, other pediatric and adult brain tumors, and normal brain tissues. Gp3, Group 3; GrpA, Group A EPN (GrpA_2 and GrpB_2 are first recurrences); ped, pediatric; SHH, sonic hedgehog; ST, supratentorial.

Constitutively activated STAT3 in EPN has pro-proliferative and antiapoptotic roles

Having identified a potentially critical role for constitutively activated STAT3 in EPN, we examined proliferation and survival of EPN cells after loss of STAT3. Functional studies were performed using an EPN cell line that was recently established from the fourth recurrence in a child with metastatic posterior fossa anaplastic EPN that exhibited a Group A phenotype. This cell line (811) was validated by karyotype analysis and was shown to harbor chromosome 1q-gain ($1q^+$), a known poor risk factor for EPN (21). Characterization of these EPN cells demonstrated that 811 secreted comparable amounts of IL6 as secreted by GBM cell line U87, in which aberrant IL6/STAT3 pathway activation had previously been identified and associated with invasiveness (ref. 22; Fig. 3A).

Loss of STAT3 through shRNA knockdown (Fig. 3B) resulted in significant reduction in proliferation of 811 cells than NT control shRNA (shNT) as measured by both cell-viability measurement (MTS) and DNA synthesis (3H-thymidine; Fig. 3C and D). Pharmacologic STAT3 inhibition (S3I-201) showed that 811 cells were more sensitive (viability IC_{50} = 108 μmol/L; DNA synthesis IC_{50} = 86 μmol/L) than U87 cells (viability IC_{50} = 140 μmol/L; DNA synthesis IC_{50} = 225 μmol/L; Supplementary Fig. S5A and S5B). The clinical relevance of these S3I-201 IC_{50} values is unknown, as S3I-201 has not yet been tested in a clinical trial, rather this inhibitor provides proof-of-principle for therapeutic targeting of STAT3. STAT3 inhibition did not affect cell cycle in 811 cells (Supplementary Fig. S5C). However, shRNA knockdown of STAT3 resulted in activation of apoptosis, with significant increase of cleaved caspase 3/7 compared with shNT (Fig. 3E), and significant apoptosis was demonstrated using S3I-201 at >IC_{50} concentration (Supplementary Fig. S5D). Collectively, these data support the hypothesis that, in EPN with constitutively activated STAT3, this transcription factor has both prosurvival and anti-apoptotic roles.

We observed an S3I-201 dose-dependent reduction of pSTAT3 pathway protein levels by Western blot (Supplementary Fig. S5E). Although total STAT3 remained relatively constant up to 500 μmol/L of S3I-201, phosphorylation was completely inhibited above 125 μmol/L. STAT3 transcriptional targets SOCS3 and MCL-1 were similarly reduced in a dose-dependent manner. STAT3 inhibition did not, however, reduce secretion of IL6, suggesting that IL6 regulation is upstream of STAT3 in the signaling pathway (Fig. 3F; Supplementary Fig. S5F).

EPN-secreted IL6 induces $CD14^+$ monocytes to secrete key proinflammatory cytokine IL8

Transcriptomic analyses of Group A EPN identified that tumor-infiltrating myeloid cells contributed strongly to the inflammatory phenotype, and specifically *IL8* expression, a hallmark of the IL6/STAT3 inflammation signature geneset, was highly enriched

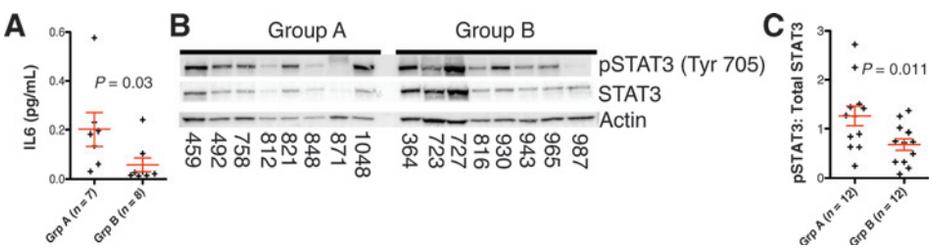

Figure 2.
Group A EPN patients have higher levels of IL6 production and a higher ratio of pSTAT3 than Group B patients. A, concentration of IL6 secretion from flow-sorted disaggregated tumor samples is higher in group A (FC = 3.5; P = 0.031, 1-tailed t test). Cells were cultured for 96 hours in O15 and normalized to 10^6 cells. B, representative Western blot showing expression of pSTAT3 and total STAT3 in patient samples. C, Western blot validation of pSTAT3 activation in surgical samples from 12 Group A and 12 Group B EPN patients. The ratio of pSTAT3 to total STAT3 was determined by densitometric measurement of Western blot bands. This demonstrated a higher ratio of STAT3 phosphorylation in samples from Group A EPN patients (FC = 1.84; P = 0.012).

Published OnlineFirst May 12, 2015; DOI: 10.1158/2326-6066.CIR-15-0061

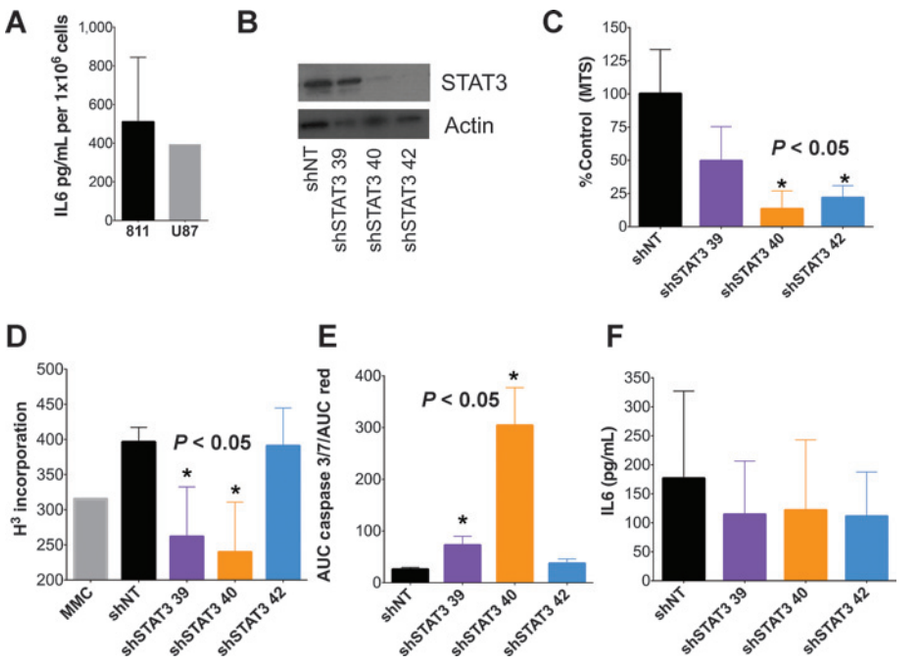

Figure 3.
EPN cell line 811 is sensitive to STAT3 knockdown leading to apoptosis. A, concentration of IL6 secretion from newly created pediatric EPN cell lines and control GBM cell line. B, Western blot validation of STAT3 knockdown in 811 cell line (representative blot). All experiments using shRNA knockdown were validated by Western blots. C and D, inhibition of cell proliferation by STAT3 knockdown was assessed by MTS and 3H-thumidine incorporation in 811 cells. Graphs are representative experiments. MMC, mitomycin C. E, real-time quantification of cleaved Caspase 3/7, representative of apoptosis, over 160 hours of STAT3 knockdown. Graph shows accumulation of cleaved caspase 3/7 normalized to cell numbers. F, IL6 secretion by 811 cells after STAT3 knockdown. *, P <0.05 calculated using 2-tailed paired t test.

in tumor-infiltrating myeloid cells (Supplementary Fig. S3). By multiplex cytokine analysis, IL6 was the predominant cytokine secreted by 811 cells, being 55-fold higher than IL8, the next highest-secreted cytokine (Supplementary Fig. S6A). No other cytokines were detected apart from trace amounts of GM-CSF, IFNγ, IL13, and IL7 (Supplementary Fig. S6A).

We hypothesized that IL6 secreted at high levels by EPN in the TME polarize tumor-infiltrating myeloid cells to an inflammatory phenotype in a paracrine fashion, resulting in activation of myeloid cell STAT3 and upregulation of transcriptional targets, including IL8. To evaluate this, $CD14^+$ monocytes were isolated from tumor HLA-matched peripheral blood mononuclear cells by flow sorting and were immediately cultured in 250 μL of either (i) 811CM, or (ii) O15 control media, for 96 hours. Supernatant from the $CD14^+$ monocyte cultures was then subject to multiplex cytokine analysis. Background cytokine levels in CM were subtracted from $CD14^+$ monocyte/CM culture cytokine levels to identify changes in monocyte-derived cytokines. There was a 9.2-fold increase ($P = 0.043$) in IL8 secretion from $CD14^+$ cells treated with 811CM compared with that with media control alone (Fig. 4A). The remaining 12 cytokines tested did not show any significant differences (data not shown).

To determine whether IL8 production in $CD14^+$ monocytes was induced by EPN-derived IL6, the experiment was repeated with the addition of IL6-neutralizing antibody (IL6NA) or IL6 receptor–neutralizing antibody tocilizumab. In both cases, production of IL8 by monocytes was significantly lowered by greater than 75% (Fig. 4B). Furthermore, flow cytometric measurement of pSTAT3 demonstrated significant induction of STAT3 phosphorylation (Tyr-705) in $CD14^+$ monocytes, and this was reversed with addition of IL6NA (Fig. 4C and D). EGF, a potential alternative activator of STAT3, was shown not to drive STAT3 phosphorylation or IL8 release, as EGFR-blocking antibody cetuximab did not reverse this phenotype in 811 CM–treated myeloid cells (Supplementary Fig. S6B and S6C). Together, these data support our hypothesis that Group A EPN secretes IL6, which stimulates production of proinflammatory IL8 by myeloid cells via activation of STAT3 in the TME in a paracrine fashion.

IL8-mediated signaling between monocytes perpetuates inflammatory signaling in the TME

IL8 is a potent chemokine that has a variety of roles in inflammation. Although its most common function is to induce neutrophil infiltration, IL8 can also promote tumor-associated macrophages to secrete more cytokines and growth factors that further induce proliferation and tumor invasion (23). IL8 was the only cytokine we found to be significantly upregulated by monocytes in response to tumor cell paracrine signaling (Fig. 4A). We hypothesized that IL8 production by tumor-polarized monocyte could further polarize monocytes in a paracrine fashion. To test this hypothesis, freshly sorted $CD14^+$ monocytes were cultured in media harvested from $CD14^+$ monocytes that had been primed in either tumor-conditioned media (MonoCM) or control media (MonoO15) for 96 hours. Strikingly, a significant upregulation of CD163 was observed in cells cultured in MonoCM compared with those cultured in control media (Fig. 5A). In addition, MonoCM induced secretion of a number of common proinflammatory cytokines IL10, IL13, IL1β, IL6, IL7, and IL8 (Fig. 5B). Addition of IL8-neutralizing antibody to MonoCM prevented CD163 upregulation and was accompanied with upregulation of both HLA-DR and Fc-receptor CD64 expression (Fig. 5A). All proinflammatory cytokine production was reduced with the addition of IL8-neutralizing antibody to MonoCM (Fig. 5B).

Collectively, these studies provide evidence that EPN tumor cells induce paracrine polarization of monocytes through secretion of IL6. This inflammatory phenotype is then amplified between monocytes through upregulated IL8 production.

Published OnlineFirst May 12, 2015; DOI: 10.1158/2326-6066.CIR-15-0061

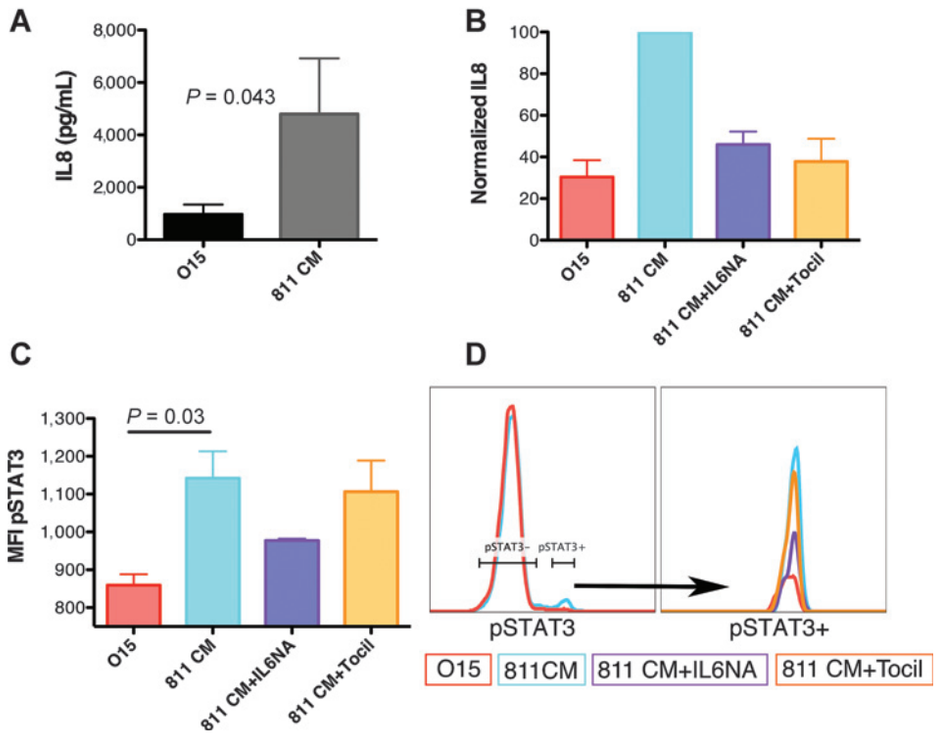

Figure 4.
EPN cell line 811 can induce immunosuppressive phenotype in HLA-matched donor CD14$^+$ peripheral blood mononuclear cells. A, IL8 secretion from HLA-matched donor CD14$^+$ monocytes incubated for 96 hours in either control media (O15) or media collected from 811 cell line (811 CM). IL8 concentration in pg/mL per 30,000 cells in 250 mL. Experiments were completed in triplicate. *P* value calculated using 1-tailed *t* test. B, IL8 secretion from CD14$^+$ monocytes incubated for 96 hours in O15, 811 CM, 811 CM plus 50 μg/mL IL6-neutralizing Ab (811 CM + IL6NA), 811 CM plus 100 μg/mL tocilizumab (811 CM + Tocil). Experiments were run in triplicate and normalized to 811 CM–cultured monocytes for each experiment. C, median fluorescence intensity (MFI) of pSTAT3 from CD14$^+$ monocytes incubated. Representative flow plot of (left) pSTAT3 for 811CM and control-treated CD14$^+$ monocytes, and (right) representative flow plot of pSTAT3-positive peak in all treatment conditions. *P* value calculated using a 1-tailed *t* test.

Discussion

Inflammatory response has been identified as a predominant transcriptomic phenotype in Group A EPN (1–3). The present study identifies tumor IL6/STAT3 pathway activation and cross-talk with myeloid cells as a potential mechanism underlying this phenotype. IL6/STAT3-mediated cross-talk between tumor and immune cells, resulting in inflammation, has been well documented in a number of tumors (20). Persistent IL6/STAT3 pathway activation is involved in various inflammation-associated cancers, most notably colorectal (14), gastric (15), and liver (16) cancers. It is known that oncogenic activation of STAT3, driven by IL6, increases cell proliferation, survival, and invasion as well as suppressing antitumor immunity (13). Tumor-derived IL6 affects the differentiation of myeloid lineages, including macrophages and dendritic cells, through STAT3 activation in these immune cell types (24). STAT3 activation in tumor-associated myeloid cells results in expression of procancer inflammatory mediators and upregulation of angiogenic factors and growth factors, leading to increased tumor growth in a paracrine fashion (20). In this study, EPN tumor cells were shown to release IL6, which activated myeloid cell STAT3 in a paracrine fashion. STAT3 activation resulted in increased IL8 production, which further polarizes myeloid cells to an inflammatory phenotype.

In the central nervous system, oncogenic IL6/STAT3 signaling has been documented predominantly in GBM, the most common malignant brain tumor in adults, as important in proliferation, survival, and invasiveness of tumor cells and as a key regulator of the immunosuppressive microenvironment (25–29). GBM have been demonstrated to harbor protumor microglia/macrophages that are polarized by glioma stem cell–secreted factors (30). This cross-talk has been attributed to STAT3 activation (31). Therapeutic targeting of STAT3 has also shown promise in the most common malignant pediatric brain tumor, MED (17, 32). To our knowledge, the present study represents the only demonstration of such cross-talk in EPN. Given that *IL6* and *IL8* gene expression is elevated in Group A EPN when compared with other brain tumors, including GBM and MED, it emphasizes the particular importance of IL6/STAT3 signaling and immune cross-talk in the biology of this tumor.

The EPN Group A IL6/STAT3 activation geneset includes critical effectors of the key phenotypic characteristics of Group A EPN (1–3), namely inflammation [*IL8*, *CCL2*, *PTGS2* (*COX2*)], mesenchymal transition (*CHI3L1*), invasiveness (*TIMP1*, *MMP2*, *MMP9*), angiogenesis (*VEGFA*), and antiapoptosis (*MCL1*, *BIRC3*). Thus, constitutive IL6/STAT3 signaling may underlie a number of the characteristic oncogenic phenotypes of Group A EPN, representing a "molecular hub" as has previously been ascribed to STAT3 in gliomas (33). A recent epigenomic study of EPN revealed that Group A, unlike Group B, exhibits a CpG island methylator phenotype (CIMP), suggesting epigenetic modifiers as rational therapeutic candidates in this molecular subgroup (34). Both IL6 and STAT3 have been shown to drive hypermethylation, potentially linking the IL6/STAT3 pathway with CIMP in this subgroup (35–37). Given these potentially pivotal roles of IL6/STAT3 in Group A EPN tumor biology, therapeutic exploration of STAT3 and/or IL6 inhibition is warranted.

We have previously shown that immunity affects outcome in pediatric EPN (19). Subsequently, we characterized immunologic differences in posterior fossa EPN, identifying an immunosuppressed phenotype in Group A when compared with Group B (3). Specifically, T cells derived from Group A tumors did not respond to stimulation with appropriate cytokine release and appeared to

Published OnlineFirst May 12, 2015; DOI: 10.1158/2326-6066.CIR-15-0061

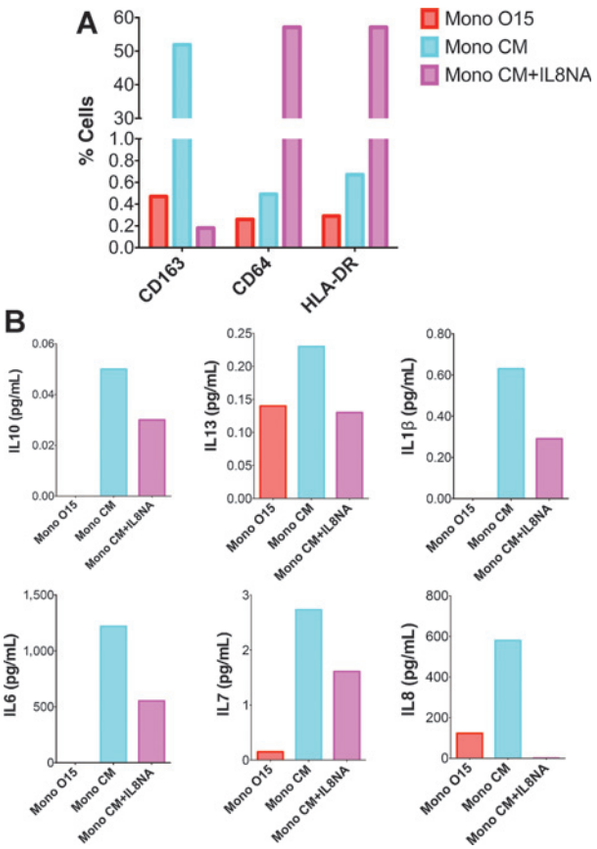

Figure 5.
IL8 secreted by EPN-polarized macrophages induces further M2-like polarization of monocytes. $CD14^+$ monocytes were incubated in O15 or 811 CM as previously described in Fig. 4. Media were then used to incubate another set of $CD14^+$ monocytes (MonoO15, MonoCM). IL8-neutralizing antibody (MonoCM+IL8NA) was used at 5 μg/mL. A, flow cytometry evaluation of cell surface markers on $CD14^+$ monocytes after incubation in media collected from EPN tumor–primed monoctyes. Graphs are percentage myeloid cells. B, concentration of cytokines secreted by monocytes from A. Cytokine already present in the media from initial polarization was subtracted to reflect additional cytokine production in pg/mL.

have an exhausted phenotype compared with those derived from Group B tumors, a finding also seen in GBM (38). Thus, in Group A EPN, there is an association of IL6/STAT3-mediated inflammation with an immunosuppressed phenotype. Numerous mechanisms have been demonstrated to link inflammation to immunosuppression, such as generation of myeloid-derived suppressive cells (39) and immunosuppressive T-cell subsets (40). STAT3 has been shown to inhibit expression of antitumor T_H1-type immune-stimulating molecules, and promote expression of immunosuppressive factors, and is therefore likely drives immunosuppression in Group A EPN (41). With the recent success of cancer therapies that inhibit immunosuppressive factors, most notably CTLA-4 and PD-1 (42, 43), identification of a tumor-associated myeloid cell–mediated immunosuppressive mechanism in Group A EPN has particular clinical relevance. Reversal of myeloid cell–mediated immunosuppressive phenotypes for therapeutic gain has been achieved by T-cell activation strategies, such as IL12 treatment that results in reprogramming of tumor-associated myeloid cells (44). Alternatively, directly targeting tumor-associated myeloid cells has shown promise, as achieved by CSF-1R inhibition in GBM (45). The ability of IL6 receptor antagonist tocilizumab, which is FDA approved for treatment of rheumatoid arthritis (46), to abrogate IL6/STAT3-mediated tumor/myeloid cell cross-talk in the present study provides yet another therapeutic approach. Group A EPN has a poor outcome and little evidence that it is responsive to standard chemotherapy. Our work is highly suggestive that in the realm of pediatric brain tumors, this specific subgroup of EPN would be a strong candidate for the development of immunotherapy.

Disclosure of Potential Conflicts of Interest

R. Vibhakar reports receiving commercial research support from Epizyme. No potential conflicts of interest were disclosed by the other authors.

Authors' Contributions

Conception and design: A.M. Griesinger, A.M. Donson, L.M. Hoffman, R. Vibhakar, N.K. Foreman

Development of methodology: A.M. Griesinger, R.J. Josephson, A.M. Donson, J.M.M. Levy, S.L. Furtek, P. Reigan, N.K. Foreman

Acquisition of data (provided animals, acquired and managed patients, provided facilities, etc.): A.M. Griesinger, A.M. Donson, J.M.M. Levy, V. Amani, L.M. Hoffman, R. Vibhakar, N.K. Foreman

Analysis and interpretation of data (e.g., statistical analysis, biostatistics, computational analysis): A.M. Griesinger, A.M. Donson, J.M.M. Levy, D.K. Birks, R. Vibhakar, N.K. Foreman

Writing, review, and/or revision of the manuscript: A.M. Griesinger, A.M. Donson, J.M.M. Levy, L.M. Hoffman, S.L. Furtek, P. Reigan, M.H. Handler, N.K. Foreman

Administrative, technical, or material support (i.e., reporting or organizing data, constructing databases): A.M. Griesinger, A.M. Donson, M.H. Handler

Study supervision: A.M. Donson, N.K. Foreman

Acknowledgments

The authors thank Dr. Hideho Okada (UCSF) and Dr. Karim El Kasmi (UCDenver) for assistance with this study.

Grant Support

This work was supported by the NIH (RO1 CA140614), NIH/NICHD (K12 HD068372), and the Tanner Seebaum Foundation. The Flow Cytometry Core Facility receives direct funding support from the NCI through the University of Colorado Cancer Center Support Grant (P30CA046934).

The costs of publication of this article were defrayed in part by the payment of page charges. This article must therefore be hereby marked *advertisement* in accordance with 18 U.S.C. Section 1734 solely to indicate this fact.

Received March 3, 2015; accepted May 3, 2015; published OnlineFirst May 12, 2015.

References

1. Witt H, Mack SC, Ryzhova M, Bender S, Sill M, Isserlin R, et al. Delineation of two clinically and molecularly distinct subgroups of posterior fossa ependymoma. Cancer Cell 2011;20:143–57.
2. Wani K, Armstrong TS, Vera-Bolanos E, Raghunathan A, Ellison D, Gilbertson R, et al. A prognostic gene expression signature in infratentorial ependymoma. Acta Neuropathol 2012;123:727–38.
3. Hoffman LM, Donson AM, Nakachi I, Griesinger AM, Birks DK, Amani V, et al. Molecular sub-group-specific immunophenotypic changes are associated with outcome in recurrent posterior fossa ependymoma. Acta Neuropathol 2014;127:731–45.
4. Grivennikov SI, Greten FR, Karin M. Immunity, inflammation, and cancer. Cell 2010;140:883–99.

Published OnlineFirst May 12, 2015; DOI: 10.1158/2326-6066.CIR-15-0061

5. Hanahan D, Weinberg RA. Hallmarks of cancer: the next generation. Cell 2011;144:646–74.
6. Diakos CI, Charles KA, McMillan DC, Clarke SJ. Cancer-related inflammation and treatment effectiveness. Lancet Oncol 2014;15:e493–e503.
7. Wu Z, Irizarry RA, Gentleman R, Martinez-Murillo F, Spencer F. A model-based background adjustment for oligonucleotide expression arrays. J Am Stat Assoc 2004;99:909–17.
8. Edgar R, Domrachev M, Lash AE. Gene Expression Omnibus: NCBI gene expression and hybridization array data repository. Nucleic Acids Res 2002;30:207–10.
9. Brunet JP, Tamayo P, Golub TR, Mesirov JP. Metagenes and molecular pattern discovery using matrix factorization. Proc Natl Acad Sci U S A 2004;101:4164–9.
10. Subramanian A, Tamayo P, Mootha VK, Mukherjee S, Ebert BL, Gillette MA, et al. Gene set enrichment analysis: a knowledge-based approach for interpreting genome-wide expression profiles. Proc Natl Acad Sci U S A 2005;102:15545–50.
11. Siddiquee K, Zhang S, Guida WC, Blaskovich MA, Greedy B, Lawrence HR, et al. Selective chemical probe inhibitor of Stat3, identified through structure-based virtual screening, induces antitumor activity. Proc Natl Acad Sci U S A 2007;104:7391–6.
12. Griesinger AM, Birks DK, Donson AM, Amani V, Hoffman LM, Waziri A, et al. Characterization of distinct immunophenotypes across pediatric brain tumor types. J Immunol 2013;191:4880–8.
13. Yu H, Pardoll D, Jove R. STATs in cancer inflammation and immunity: a leading role for STAT3. Nat Rev Cancer 2009;9:798–809.
14. Belluco C, Nitti D, Frantz M, Toppan P, Basso D, Plebani M, et al. Interleukin-6 blood level is associated with circulating carcinoembryonic antigen and prognosis in patients with colorectal cancer. Ann Surg Oncol 2000;7:133–8.
15. Ashizawa T, Okada R, Suzuki Y, Takagi M, Yamazaki T, Sumi T, et al. Clinical significance of interleukin-6 (IL-6) in the spread of gastric cancer: role of IL-6 as a prognostic factor. Gastric Cancer 2005;8:124–31.
16. Giannitrapani L, Cervello M, Soresi M, Notarbartolo M, La Rosa M, Virruso L, et al. Circulating IL-6 and sIL-6R in patients with hepatocellular carcinoma. Ann New York Acad Sci 2002;963:46–52.
17. Xiao H, Bid HK, Jou D, Wu X, Yu W, Li C, et al. A novel small molecular STAT3 inhibitor, LY5 inhibits cell viability, cell migration, and angiogenesis in medulloblastoma cells. J Biol Chem 2015;290:3418–29.
18. McFarland BC, Hong SW, Rajbhandari R, Twitty GB Jr, Gray GK, Yu H, et al. NF-kappaB-induced IL-6 ensures STAT3 activation and tumor aggressiveness in glioblastoma. PLoS One 2013;8:e78728.
19. Donson AM, Birks DK, Barton VN, Wei Q, Kleinschmidt-Demasters BK, Handler MH, et al. Immune gene and cell enrichment is associated with a good prognosis in ependymoma. J Immunol 2009;183:7428–40.
20. Yu H, Kortylewski M, Pardoll D. Crosstalk between cancer and immune cells: role of STAT3 in the tumour microenvironment. Nat Rev Immunol 2007;7:41–51.
21. Mendrzyk F, Korshunov A, Benner A, Toedt G, Pfister S, Radlwimmer B, et al. Identification of gains on 1q and epidermal growth factor receptor overexpression as independent prognostic markers in intracranial ependymoma. Clin Cancer Res 2006;12:2070–9.
22. Li R, Li G, Deng L, Liu Q, Dai J, Shen J, et al. IL-6 augments the invasiveness of U87MG human glioblastoma multiforme cells via up-regulation of MMP-2 and fascin-1. Oncol Rep 2010;23:1553–9.
23. Waugh DJ, Wilson C. The interleukin-8 pathway in cancer. Clin Cancer Res 2008;14:6735–41.
24. Park SJ, Nakagawa T, Kitamura H, Atsumi T, Kamon H, Sawa S, et al. IL-6 regulates in vivo dendritic cell differentiation through STAT3 activation. J Immunol 2004;173:3844–54.
25. Haftchenary S, Luchman HA, Jouk AO, Veloso AJ, Page BD, Cheng XR, et al. Potent targeting of the STAT3 protein in brain cancer stem cells: a promising route for treating glioblastoma. ACS Med Chem Lett 2013;4:1102–7.
26. Assi H, Espinosa J, Suprise S, Sofroniew M, Doherty R, Zamler D, et al. Assessing the role of STAT3 in DC differentiation and autologous DC immunotherapy in mouse models of GBM. PLoS One 2014;9:e96318.
27. Hussain SF, Kong LY, Jordan J, Conrad C, Madden T, Fokt I, et al. A novel small molecule inhibitor of signal transducers and activators of transcription 3 reverses immune tolerance in malignant glioma patients. Cancer Res 2007;67:9630–6.
28. Abou-Ghazal M, Yang DS, Qiao W, Reina-Ortiz C, Wei J, Kong LY, et al. The incidence, correlation with tumor-infiltrating inflammation, and prognosis of phosphorylated STAT3 expression in human gliomas. Clin Cancer Res 2008;14:8228–35.
29. Fujita M, Zhu X, Sasaki K, Ueda R, Low KL, Pollack IF, et al. Inhibition of STAT3 promotes the efficacy of adoptive transfer therapy using type-1 CTLs by modulation of the immunological microenvironment in a murine intracranial glioma. J Immunol 2008;180:2089–98.
30. Wu A, Wei J, Kong LY, Wang Y, Priebe W, Qiao W, et al. Glioma cancer stem cells induce immunosuppressive macrophages/microglia. Neuro Oncol 2010;12:1113–25.
31. Li W, Graeber MB. The molecular profile of microglia under the influence of glioma. Neuro Oncol 2012;14:958–78.
32. Yang MY, Lee HT, Chen CM, Shen CC, Ma HI. Celecoxib suppresses the phosphorylation of STAT3 protein and can enhance the radiosensitivity of medulloblastoma-derived cancer stem-like cells. Int J Mol Sci 2014;15:11013–29.
33. Brantley EC, Benveniste EN. Signal transducer and activator of transcription-3: a molecular hub for signaling pathways in gliomas. Mol Cancer Res 2008;6:675–84.
34. Mack SC, Witt H, Piro RM, Gu L, Zuyderduyn S, Stutz AM, et al. Epigenomic alterations define lethal CIMP-positive ependymomas of infancy. Nature 2014;506:445–50.
35. Foran E, Garrity-Park MM, Mureau C, Newell J, Smyrk TC, Limburg PJ, et al. Upregulation of DNA methyltransferase-mediated gene silencing, anchorage-independent growth, and migration of colon cancer cells by interleukin-6. Mol Cancer Res 2010;8:471–81.
36. Zhang Q, Wang HY, Marzec M, Raghunath PN, Nagasawa T, Wasik MA. STAT3- and DNA methyltransferase 1-mediated epigenetic silencing of SHP-1 tyrosine phosphatase tumor suppressor gene in malignant T lymphocytes. Proc Natl Acad Sci U S A 2005;102:6948–53.
37. Lee H, Zhang P, Herrmann A, Yang C, Xin H, Wang Z, et al. Acetylated STAT3 is crucial for methylation of tumor-suppressor gene promoters and inhibition by resveratrol results in demethylation. Proc Natl Acad Sci U S A 2012;109:7765–9.
38. Wei J, Barr J, Kong LY, Wang Y, Wu A, Sharma AK, et al. Glioblastoma cancer-initiating cells inhibit T-cell proliferation and effector responses by the signal transducers and activators of transcription 3 pathway. Mol Cancer Ther 2010;9:67–78.
39. Marigo I, Bosio E, Solito S, Mesa C, Fernandez A, Dolcetti L, et al. Tumor-induced tolerance and immune suppression depend on the C/EBPbeta transcription factor. Immunity 2010;32:790–802.
40. Gallina G, Dolcetti L, Serafini P, De Santo C, Marigo I, Colombo MP, et al. Tumors induce a subset of inflammatory monocytes with immunosuppressive activity on CD8+ T cells. J Clin Invest 2006;116:2777–90.
41. Wang T, Niu G, Kortylewski M, Burdelya L, Shain K, Zhang S, et al. Regulation of the innate and adaptive immune responses by Stat-3 signaling in tumor cells. Nat Med 2004;10:48–54.
42. Hodi FS, O'Day SJ, McDermott DF, Weber RW, Sosman JA, Haanen JB, et al. Improved survival with ipilimumab in patients with metastatic melanoma. N Engl J Med 2010;363:711–23.
43. Topalian SL, Hodi FS, Brahmer JR, Gettinger SN, Smith DC, McDermott DF, et al. Safety, activity, and immune correlates of anti-PD-1 antibody in cancer. N Engl J Med 2012;366:2443–54.
44. Kerkar SP, Goldszmid RS, Muranski P, Chinnasamy D, Yu Z, Reger RN, et al. IL-12 triggers a programmatic change in dysfunctional myeloid-derived cells within mouse tumors. J Clin Invest 2011;121:4746–57.
45. Pyonteck SM, Akkari L, Schuhmacher AJ, Bowman RL, Sevenich L, Quail DF, et al. CSF-1R inhibition alters macrophage polarization and blocks glioma progression. Nat Med 2013;19:1264–72.
46. Genovese MC, McKay JD, Nasonov EL, Mysler EF, da Silva NA, Alecock E, et al. Interleukin-6 receptor inhibition with tocilizumab reduces disease activity in rheumatoid arthritis with inadequate response to disease-modifying antirheumatic drugs: the tocilizumab in combination with traditional disease-modifying antirheumatic drug therapy study. Arthritis Rheum 2008;58:2968–80.

Published OnlineFirst May 12, 2015; DOI: 10.1158/2326-6066.CIR-15-0061

Cancer Immunology Research

Interleukin-6/STAT3 Pathway Signaling Drives an Inflammatory Phenotype in Group A Ependymoma

Andrea M. Griesinger, Rebecca J. Josephson, Andrew M. Donson, et al.

Cancer Immunol Res 2015;3:1165-1174. Published OnlineFirst May 12, 2015.